Quinolimide-based peptide biosensor for probing p25 in vitro and in living cells

Francisco Fueyo-González, Rosario Herranz, Simona Plesselova, Maria Giron, Rafael Salto, Jose Manuel Paredes, Angel Orte, May C Morris, Juan González-Vera

Quinolimide-based peptide biosensor for probing p25 *in vitro* and in living cells

Francisco Fueyo-González[a,e], Rosario Herranz[a], Simona Plesselova[b], Maria D. Giron[b], Rafael Salto[b], Jose Manuel Paredes[c], Angel Orte[c], May C. Morris[d,*], and Juan A. González-Vera[a,c,d,*]

[a]*Instituto de Química Médica (CSIC). Juan de la Cierva 3, 28006 Madrid, Spain.*

[b]*Departamento de Bioquímica y Biología Molecular II, Facultad de Farmacia, Universidad de Granada. Campus Cartuja, 18071, Granada, Spain*

[c]*Departamento de Fisicoquímica, Unidad de Excelencia de Química Aplicada a Biomedicina y Medioambiente, Facultad de Farmacia, Universidad de Granada, Campus Cartuja, 18071, Granada, Spain.*

[d]*Institut des Biomolécules Max Mousseron, IBMM-UMR 5247, Université de Montpellier, Faculté de Pharmacie, 15 Av. Charles Flahault, 34093 Montpellier, France.*

Corresponding authors E-mail addresses: gonzalezvera@ugr.es (J. A. González-Vera); may.morris@umontpellier.fr (M. Morris)

ABSTRACT

CDK5 kinase is activated through interactions with different partners including the p35/p25 regulators. Active CDK5 plays a key role in several neuronal functions and its hyperactivity contributes to a variety of neurodegenerative processes and several human cancers, in particular glioblastomas and neuroblastomas. In order to probe partners that interact with CDK5, we designed and synthesized fluorescent quinolimide-labelled peptides derived from the C-helix of CDK5, which were implemented to probe CDK5 partners *in vitro* and by *in cellulo* imaging in U87 glioblastoma and N2a

[e]Current address: Department of Medicine, Translational Transplant Research Center, Immunology Institute, Icahn School of Medicine at Mount Sinai, New York, USA.

neuroblastoma cells. Ectopic expression of a NIR fluorescent protein miRFP670 fusion with p25 (p25-miRFP670) in N2a cells induced FRET between a quinolimide-labelled peptide biosensor and p25-miRFP670, and fluorescence intensity was proportional to the expression level of p25, thereby demonstrating the potential of the quinolimide-labelled peptide biosensor to report on p25 relative abundance.

Keywords: Fluorescence probes; Quinolimide derivatives; CDK5; p25 sensors; FRET imaging; Protein-protein interactions.

1. Introduction

CDK5 is a serine/threonine kinase, member of the cyclin-dependent kinase (CDK) family, which is expressed ubiquitously, but primarily in post-mitotic neurons, where it is activated by the neurospecific activators p35/p25 and p39/p29 [1]. CDK5 has also been reported to interact with several cyclin partners, including cyclins E, I and Y [2]. CDK5 is mostly present in the central nervous system, where it induces the extension of neurites, neuronal maturation, synapse formation in brain development, synaptic plasticity, axonal guidance, neuronal development and differentiation, and is involved in autophagy regulation [3, 4]. CDK5 activation occurs after the proteolytic cleavage of p35 or p39 protein partners to p25 or p29, by calpain and stimulated by Ca^{2+}, which is released into the cytoplasm [5, 6]. p25 does not present sequence similarity with cyclins, but adopts a similar fold and binds to CDK5 at the same interface as other CDKs bind cyclins, known as the C-helix.

CDK5 hyperactivity is related with the onset and development of several neurodegenerative diseases, inducing neuronal death [3, 7-9]. Diverse studies have demonstrated the involvement of the CDK5 hyperactivation by p25 in Alzheimer's disease, Parkinson's disease and amyotrophic lateral sclerosis (ALS). In fact, CDK5 participates in phosphorylation of tau protein [9-11]. It also contributes to hyperphosphorylation of α-synuclein and parkin, and to the consequent generation of Lewy bodies in Parkinson's disease [12, 13], and further induces neuronal loss in ALS [14]. Recently, the

involvement of CDK5 in neuronal death during cerebral ischemia has also been described [15]. Furthermore, numerous studies report upregulation or hyperactivation of CDK5 in several types of human cancers, highlighting the importance of this kinase as a drug target for cancer therapy [3, 9, 16-18]. Abnormal expression or hyperactivation of CDK5 is associated with tumorigenesis and tumor progression, including cancer stem cells, by promoting proliferation, migration and angiogenesis. CDK5 activity participates in control of the DNA damage pathway, resistance to cancer chemotherapy and anti-tumor immunity [16, 17]. In particular, recent studies suggest that the expression and hyperactivity of this kinase are involved in the development and degree of aggressiveness of glioblastomas and neuroblastomas [19, 20]. CDK5 is an invaluable tumorigenesis and glioma progression biomarker [20]. Therefore, CDK5 constitutes an attractive pharmacological target in neurodegenerative disorders (Parkinson's, Alzheimer's, Huntington's and ALS) and oncology. Hence development of a fluorescent biosensor of CDK5 partners involved in its activation would constitute an attractive means of reporting on aberrant or excessive interactions of CDK5 with its partners and its potential dysregulation in pathological conditions.

Environment-sensitive fluorophores and in particular solvatochromic dyes have been commonly employed in the development of biosensors for probing protein-protein interactions [21, 22]. Photophysical properties (e.g. emission wavelengths, quantum yields and fluorescence lifetimes) of these dyes are highly dependent on the polarity of their neighboring environment, exhibiting, in general, very low fluorescence emission in water and polar solvents, in contrast to that in non-polar environments. This high sensitivity to their surrounding microenvironment makes them suitable for reporting on molecular interactions with high signal-to-noise ratio. Since the interfaces of protein-protein interactions are usually hydrophobic, solvatochromic fluorophores sense these interactions through significant increases in fluorescence, relative to their free exposure to the solvent.

In this field, we have described a new family of highly solvatochromic and fluorogenic fluorophores based on a 9-methoxy-quinolimide scaffold (Figure 1, **A**), which demonstrated sensitivity for probing partners of CDK5 in glioblastoma cells [23]. The photophysical properties of

these fluorophores have been improved by replacing the electron donor 9-methoxy group by diverse amino groups (Figure 1, **B**). Among the studied amino groups, quinolimides with a methylamino or the cyclic amine azetidine showed the best photophysical properties. Specifically, 9-azetidinyl-5-butyl-quinolimide (Figure 1, **B**: R = *n*Bu, R^1 = azetidine) has demonstrated high potential for *in vivo* sensing β-amyloid aggregation in a zebrafish model, enabling to identify the appearance of different types of early pre-amyloid oligomers [24]. In view of the solvatochromic and fluorogenic behavior of 9-methylamino and 9-azetidinyl-quinolimides, we decided to prepare bromoacetamide derivatives of these fluorophores as peptide labelling reagents and to implement their use to develop a CDK5-based peptide biosensor of p25 level by FRET imaging in cultured cells.

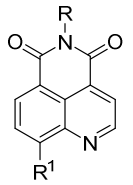

A: R^1 = OMe
B: R^1 = NR^2R^3

Figure 1. General structure of quinolimide-based fluorophores.

2. Experimental Section

2.1. Synthetic Materials and Methods

Complete information on the synthesis, photophysical and NMR characterization data of quinolimides **2–5** (see Scheme 1) has been included in the Supplementary Material, as well as peptide labelling and titration experiments.

*2.2. Colocalization of quinolimide labelled biosensor (Pep1-K5-**5**) with endogenous p25 in U87 glioblastoma cells*

A previously reported protocol was followed [23]. Pep1-CDK5 peptide labelled with **5** (Pep1-K5-**5**, 2 μM) was added to U87 cells. Indirect immunofluorescence was carried out with rabbit polyclonal

anti-p25 using Alexa Fluor 647-conjugated secondary antibodies and nuclei were stained with Hoechst. Cells were visualized using a Zeiss microscope with a CoolSnap camera and images were obtained with MetaMorph software.

2.3. Generation of a eukaryotic expression vector for p25 fused to the miRFP660 fluorescent protein (pmiRFP670-N-P25)

p25 coding sequence was amplified by PCR from plasmid GST-p25 (a gift from Harish Pant, Addgene plasmid # 24896) that encodes for a truncated version of p35 protein [25]. p25 sequence, without the stop codon was amplified from GST-p25 by PCR using *Pfu* polymerase and primers including a 5´*BamH*I and 3´*EcoR*I restriction sites. In addition, the forward primer included a Kozak sequence plus an initiation codon (Forward primer: 5´-ggatcccaccatgGCCCAGCCCCCGCCG-3´ and Reverse primer: 5´-GaattcgCCGATCCAGGCCTAGGAG-3´ where the lowercase letters correspond to the restriction sites, kozak sequence and initiation codon added). The PCR fragment was subcloned using *BamH*I and 3´*EcoR*I restriction sites into the *Bgl*II and *EcoR*I restriction sites in the pmiRFP670-N1 vector (a gift from Vladislav Verkhusha, Addgene plasmid # 79987), a eukaryotic expression vector that encodes the monomeric near-infrared fluorescent protein miRFP670 [26]. The resulting plasmid was termed pmiRFP670-N-p25 and its sequence was confirmed by automatic sequencing.

2.4. In cellulo probing expression levels of p25 in N2a cells using dual-color ratiometric and fluorescence lifetime (FLIM) imaging

Murine neuroblastoma Neuro-2a cells (N2a; ATCC No. CCL-131) were cultured in Dulbecco's Modified Eagle's medium (DMEM) supplemented with glutamine plus (2 mM), FBS (10 %), penicillin (100 units/mL) and streptomycin (0.1 mg/mL) in a CO_2 atmosphere (5 %). Prior to transfection either with plasmid pmiRFP670-N-P25 or pmiRFP670-N1, cells were seeded onto coverslips in 6 well plates at a density of 2.3×10^5 cells/well for 24 h to obtain an 80–90 % cell confluence. For transfection experiments, pmiRFP670-N1 and pmiRFP670-N-P25 plasmids (4.3 μg/well) were mixed with LP2000 (10 μL) for 30 min at room temperature (100 μL of total volume).

Next, the mixture was diluted with DMEM (without FBS) to 1 mL and added to the wells. Cells were added the polyplexes and incubated for 5 h. Afterwards medium was removed and cells were grown in DMEM plus FBS (10 %) for 24 h. Transfected cells were used for fluorescence microscopy and image analysis. For differentiation experiments, medium was replaced with DMEM supplemented with 1% FBS for 24h. For the experiments using rosiglitazone, N2a cells were treated with rosiglitazone 200 µM for 24h.

2.5. Dual-color FLIM studies

Dual-color FLIM was performed on a MicroTime 200 system (PicoQuant GmbH) as previously described [24]. Two pulsed interleaved excitation lasers at λ_{ex}= 470 nm and λ_{ex}= 635 nm were employed and fluorescence was split into two detection channels with a 600DCXR dichroic mirror. The green channel was defined with a 550/40 bandpass filter whereas a 685/70 bandpass filter was used for red channel. FLIM imaging analyses were carried out employing SymphoTime 32 (PicoQuant GmbH) and home-coded scripts in FiJi (distribution of ImageJ [27]).

3. Results and discussion

3.1. Synthesis of peptide labelling reagents

As shown in Scheme 1, the 9-amino quinolimides **2** and **3** were obtained by replacement of the 9-methoxy group of quinolimide **1** [23] by the corresponding amine, via aromatic nucleophilic substitution [28], under microwave activated heating at 120 ºC. After removal of the protecting Boc group from **2** and **3**, by treatment with TFA in CH_2Cl_2, the reaction at room temperature with bromoacetic acid bromide in the presence of DIPEA, as acceptor of the generated BrH, led to the corresponding bromoacetamides **4** and **5** with 82 and 32 % yield, respectively.

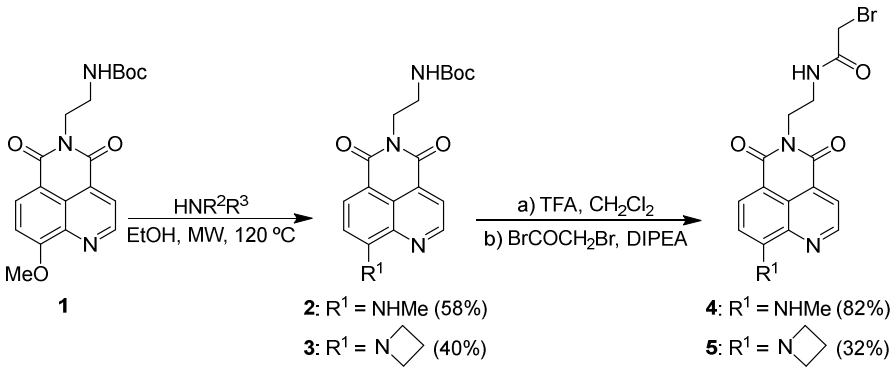

Scheme 1. Synthesis of the thiol-reactive bromoacetamides **4** and **5**.

*3.2. Photophysical properties of bromoacetamides **4** and **5***

UV absorption and fluorescence emission properties of bromoacetamide derivatives **4** and **5** were determined in dioxane, as nonpolar solvent, and water and are shown in Table 1. As expected the fluorescence emission of **4** and **5** was significantly higher in dioxane than in water, as well as their respective lifetimes. Moreover, these dyes display very large Stokes shifts (> 100 nm).

Table 1. Photophysical properties of the bromoacetamides **4** and **5**

Compd[a]	Solvent	λ_{max}^{abs} (nm)	ε ($M^{-1}cm^{-1}$)	λ_{max}^{em} (nm)	Φ_F[b]	τ(ns)[c]
4	Dioxane	463	15300 ± 1000	583	0.029 ± 0.002	1.80 ± 0.01
	H_2O	483	11100 ± 700	617	<0.001	0.20 ± 0.02
5	Dioxane	474	14200 ± 900	583	0.120 ± 0.008	3.96 ± 0.08
	H_2O	492	11200 ± 700	623	<0.001	0.68 ± 0.06

[a]Measured in duplicate at a 12 μM concentration. [b]Quantum yields calculated with reference to coumarin 153 (in EtOH). [c]Fluorescence lifetimes obtained with λ_{ex} = 485 nm, as global fits of three fluorescence decay traces collected at λ_{max}^{em}–10 nm, λ_{max}^{em}, and λ_{max}^{em}+10 nm. The reported values are the mean of the intensity-weigthed average fluorescence lifetimes at the three different wavelengths from triexponencial decay fittings. The associated error is the standard deviation of the mean.

3.3. Fluorescent peptide design, labelling and in vitro study of the CDK5/p25 interaction

As shown in Figure 3, the crystal structure of the CDK5/p25 complex shows that CDK5 binds p25 through the C-helix (PISTVRE, in red) of CDK5 and the α helix of p25 (in yellow) [29, 30]. Therefore, to study the interaction between the C-helix of CDK5 and its partners, we labelled a peptide derived from the C-helix of CDK5 (K5 peptide, GVPSSALREICLLK [23]), which bears a single cysteine residue, with the prepared bromoacetamides **4** and **5**, respectively (Figure 3c). The resulting labelled peptides K5-**4** and K5-**5** were then titrated with a peptide derived from the interacting α helix of p25 (p25-S1 peptide, KEAFWDRCLSVINLM [23]). In the absence of this peptide, the emission of peptides K5-**4** (Figure 4a) and K5-**5** (Figure 4b) was very low; however, it increased significantly in the presence of increasing concentrations of the p25-S1 peptide. Addition of p25-S1 peptide to labelled peptides K5-**4** and K5-**5** produced hypsochromic shifts of 38 and 37 nm (from red to orange) and 21.6- and 20.2-fold fluorescence emission intensity enhancement, respectively, indicative of an effective interaction with p25-S1.

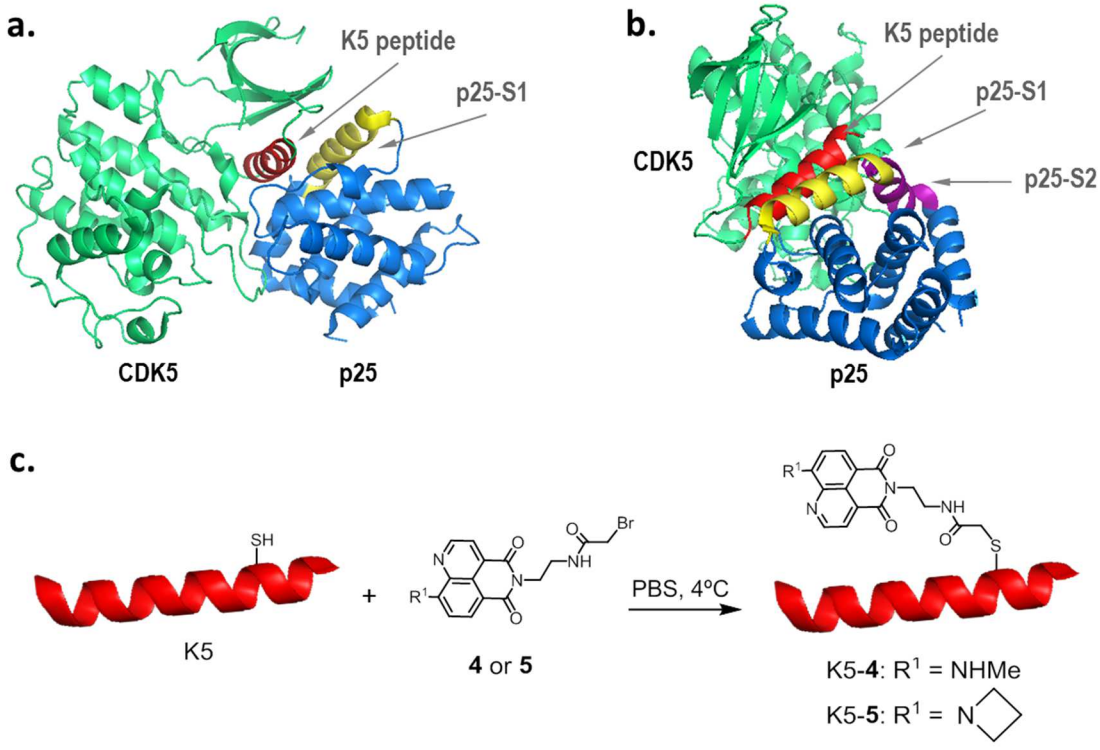

Figure 3. (a and b) Cartoon representation of the CDK5/p25 complex (PDB 1UNG), in two different poses, with the interface between CDK5 (green) and p25 (blue) mediated by contacts between the C helix of CDK5 (PSTAIRE; red), and the α helix of p25 (yellow)[30]. Color code of peptides derived from CDK5/p25 interaction employed in this work: p25-S1 peptide in yellow, p25-S2 peptide in purple and K5 peptide in red. (c) Scheme of peptide labelling.

Binding constants, K_d, were obtained through the fluorescence titration curves as described in the Supplementary Material. The K_d value for K5-**4** was 420 ± 80 μM, while K5-**5** exhibited a K_d value of 49 ± 15 μM, which, importantly, represents a 8.5-fold increase in affinity compared to that of K5-**4** and 7-fold increase respect to that of our previously reported 9-methoxy-quinolimide-based biosensor [23]. Moreover, the titration of K5-**4** and K5-**5** with an unrelated peptide (VESSDTIDNVKSKIQDKEGC [31]) (Figure S3) did not produce a fluorescence increase, demonstrating that the probe is not involved in a false interaction and, therefore, highlighting that binding of the labelled peptides is selective for the p25-S1 peptide. As a negative control, we titrated K5-**5** with a peptide derived from another α helix close to the interacting α helix of p25 but not directly involved in the CDK5/p25 interaction (p25-S2 peptide, CSKMLQINAD), which showed a negligible binding (Figure 4c; K_d > 6000 μM). Furthermore, the titration of the K5 peptide labelled with a standard fluorophore with low solvatochromic behavior, such as fluorescein (FITC), only led to 1.5-fold increase in fluorescence, with no related spectral shift (Figure S3). These results show that both K5-**4** and K5-**5** peptides constitute useful tools for studying partners that interact with the C-helix of CDK5, in particular the azetidine derivative K5-**5**, due to its greater brightness, longer excitation and emission wavelengths, larger fluorescence lifetime and greater affinity for the peptide derived from p25-S1.

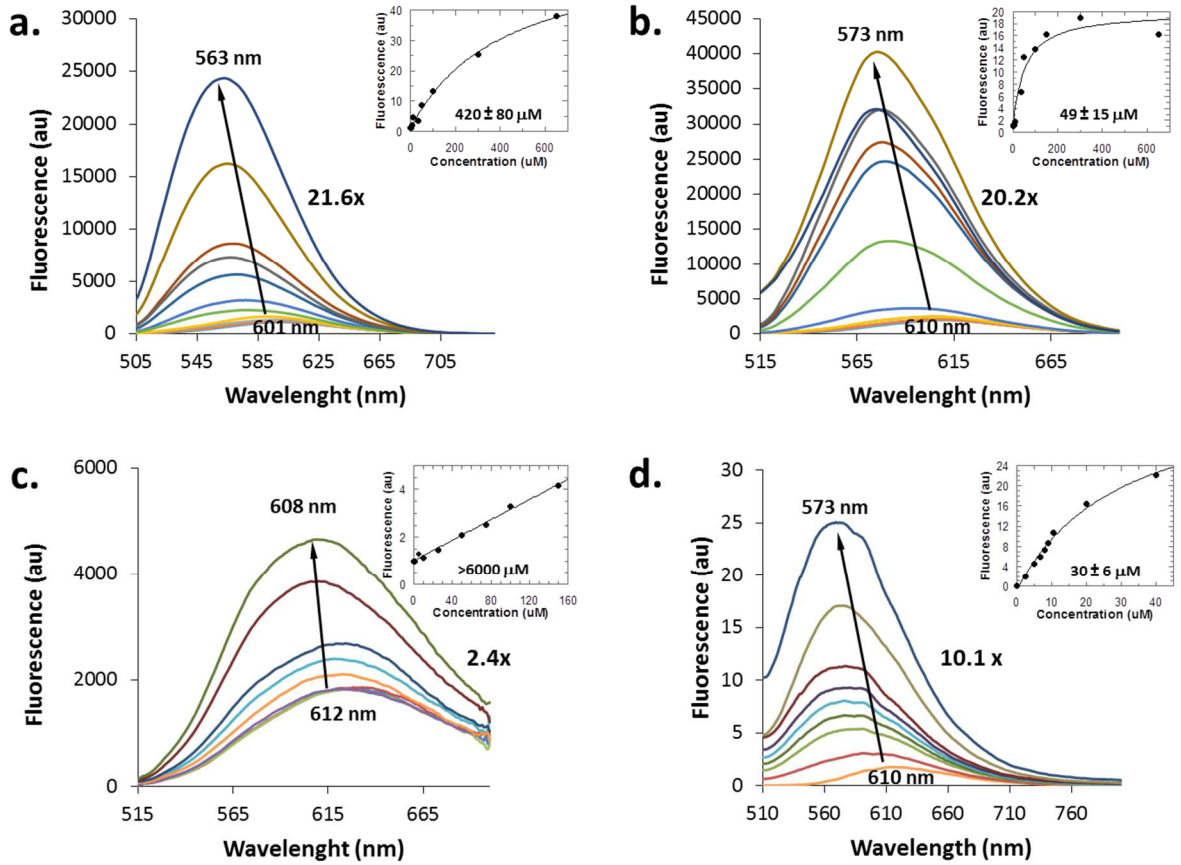

Figure 4. (a) Titration of K5-**4** (5 µM) with the p25-S1 peptide (λ_{ex}= 480 nm) and curve fit. (b) Titration of K5-**5** (5 µM) with the p25-S1 peptide (λ_{ex}= 490 nm) and curve fit. (c) Titration of K5-**5** (5 µM) with the p25-S2 peptide (λ_{ex}= 490 nm) and curve fit. (d) Titration of Pep1-K5-**5** (0.2 µM) with GST-p25 protein (λ_{ex}= 490 nm) and curve fit. Insets a-d: plots of fluorescence intensity versus concentration of the peptide. Lines represent results from non-linear curve fitting from which the binding constant, K_d, values included in the insets were obtained.

*3.4. Colocalization of quinolimide labelled biosensor (Pep1-K5-**5**) with endogenous p25 in U87 glioblastoma cells*

Next, we investigated whether K5 labelled with the 9-azetidinyl-quinolimide **5** (K5-**5**) could be used as a probe for the *in cellulo* imaging of CDK5 partners in U87 glioblastoma cells. As expected, the K5-**5** peptide, by itself, did not penetrate into cells. Therefore, a fusion of the cell-penetrating peptide Pep1 [32, 33] with the K5 peptide was synthesized and was then labelled with bromoacetamide **5**. Prior to the *in cellulo* assay, we studied the *in vitro* interaction between labelled

peptide Pep1-K5-**5** (KETWWETWWTEKKGVPSSALREIC(**5**)LLK) and recombinant GST-p25. The titration of Pep1-K5-**5** with GST-p25 led to a hypsochromic shift of 37 nm and 10.1-fold increase in fluorescence, with a K_d value of 30 ± 6 μM, which indicated an effective binding to p25 protein (Figure 4d). Pep1-K5-**5** peptide readily penetrated into living U87 cells, and its colocalization with endogenous p25 was investigated by fluorescence microscopy following indirect immunofluorescence with a p25 antibody labelled with the Alexa Fluor 647 fluorophore in U87 cells overlaid with the Pep1-K5-**5** peptide. The results showed a complete overlay of the signal of Pep1-K5-**5** observed through the GFP filter with that of Alexa Fluor 647-labelled secondary/anti-p25 primary antibodies (Figure 5a). The calculated Pearson colocalization coefficient was 0.93 ± 0.03 (Figure 5c). In contrast, cells which had not been treated with the Pep1-K5-**5** peptide did not reveal any signal through the GFP channel (Figure 5b). Remarkably, the Pep1-K5-**5** peptide led to a 6.3-fold fluorescence increase, inferring it interacts with p25 *in cellulo*. As shown in Figure 5d, this represents a significant improvement compared to our previously reported 9-methoxy-quinolimide-based CDK5 probe (Pep1-K5-**A**) [23].

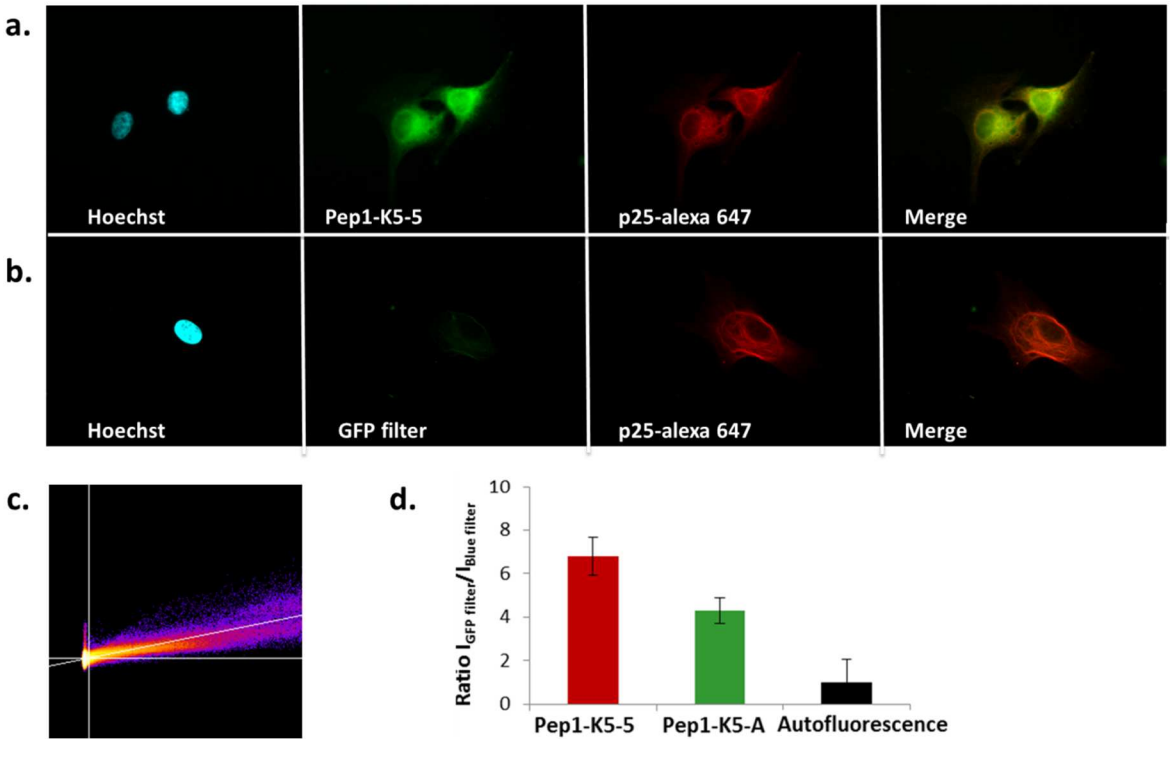

Figure 5. Colocalization of Pep1-K5-**5** with p25. (a) Indirect immunofluorescence of p25 in cells treated with Pep1-K5-**5**. (b) Indirect immunofluorescence of p25 in cells. Images in the green channel (GFP filter) appeared with negligible signal. (c) Graph representing the intensity in the two channels used to calculate Pearson colocalization coefficient. (d) Intensity ratio $I_{GFP\ filter}/I_{Blue\ filter}$ of Pep1-K5-**5** and the analogue 9-methoxy-quinolimide labelled Pep1-K5 peptide (Pep1-K5-**A**) [23].

3.5. Reporting different levels of p25 in cellulo *via FRET between Pep1-K5-**5** and ectopically expressed iRFP670-p25 in N2a neuroblastoma cells*

Finally, we decided to assess the potential of the 9-azetidinyl-quinolimide labelled peptide Pep1-K5-**5** to report on different levels and expression patterns of the p25 protein in cultured cells. For this purpose, we engineered a FRET-based system composed by our 9-amino-quinolimide labelled peptide derived from CDK5 (Pep1-K5-**5**), as FRET donor, and p25 protein fused to the NIR fluorescent fusion protein miRFP670 (p25-miRFP670), as FRET acceptor. miRFP670 was chosen based on its spectral properties [34], which ensure a suitable FRET pair with the 9-azetidinyl-quinolimide dye thanks to a good spectral overlap. In this system, when the labelled peptide Pep1-K5-**5** would bind p25-miRFP670, we hypothesized the probe would become embedded in a hydrophobic environment which would increase its fluorescence and transfer the energy to miRFP670, thereby resulting in NIR emission (Figure 6), together with a decrease in the fluorescence lifetime of **5**. The implementation of the proposed FRET system would formally demonstrate that the CDK5-derived peptide biosensor indeed recognizes and responds to differences in p25 abundance in cultured cells. Moreover it would provide the opportunity to develop an *in cellulo* screen of compounds, which might interfere with the CDK5/p25 interaction, of potential therapeutic utility.

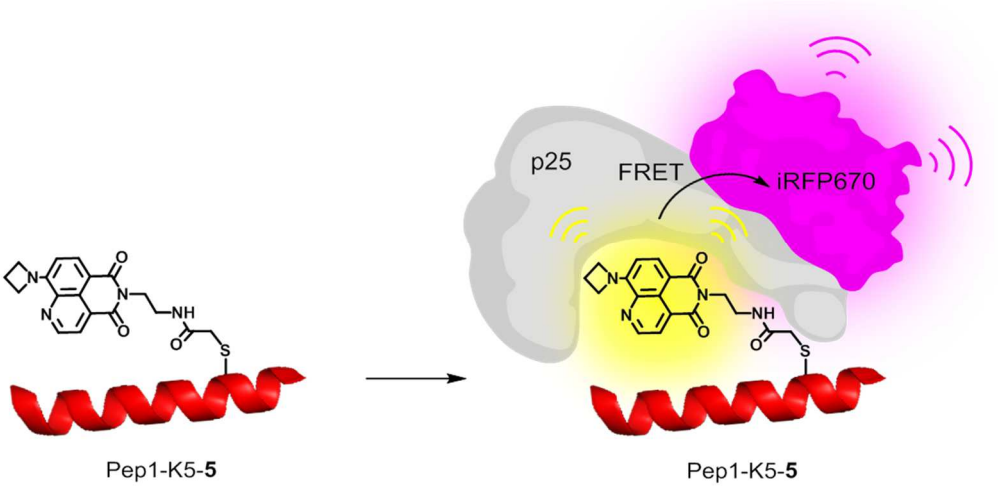

Figure 6. Schematic representation of the FRET-based biosensor for K5/p25 interaction. Upon binding of the Pep1-K5-**5** peptide to the p25-miRFP670 target protein, the donor dye **5** would transfer its excitation energy to the fluorescent fusion protein, resulting in NIR emission of the acceptor.

With this experimental design in mind, N2a neuroblastoma cells expressing physiological levels of p25 [35] were either mock-transfected or transfected with pmiRFP670-N-p25 or pmiRFP670-N1 plasmids. The N2a mock-transfected cells (cells A) as well as the pmiRFP670-N1 transfected cells (cells B) express basal, physiological levels of p25. On the contrary, the pmiRFP670-N-p25 transfected cells (cells C) overexpress p25 fused to the miRFP670 fluorescent protein. Three different microscope configurations (Figure 7) were selected in order to separate the emission of the fluorescently-labelled Pep1-K5-**5** peptide (λ_{ex} = 470 nm ,λ_{em} = 550/40 nm; Green channel, Figure 7a), the emission of the NIR protein miRFP670 (λ_{ex} = 635 nm, λ_{em} = 685/70 nm; Red channel, Figure 7b) and the last channel corresponding to the emission due to FRET (λ_{ex} = 470 nm, λ_{em} = 685/70 nm; FRET channel, Figure 7c). Importantly, we also followed the FRET process by focusing on the decrease in the donor's fluorescence lifetime by using fluorescence lifetime imaging (FLIM, Figure 7d).

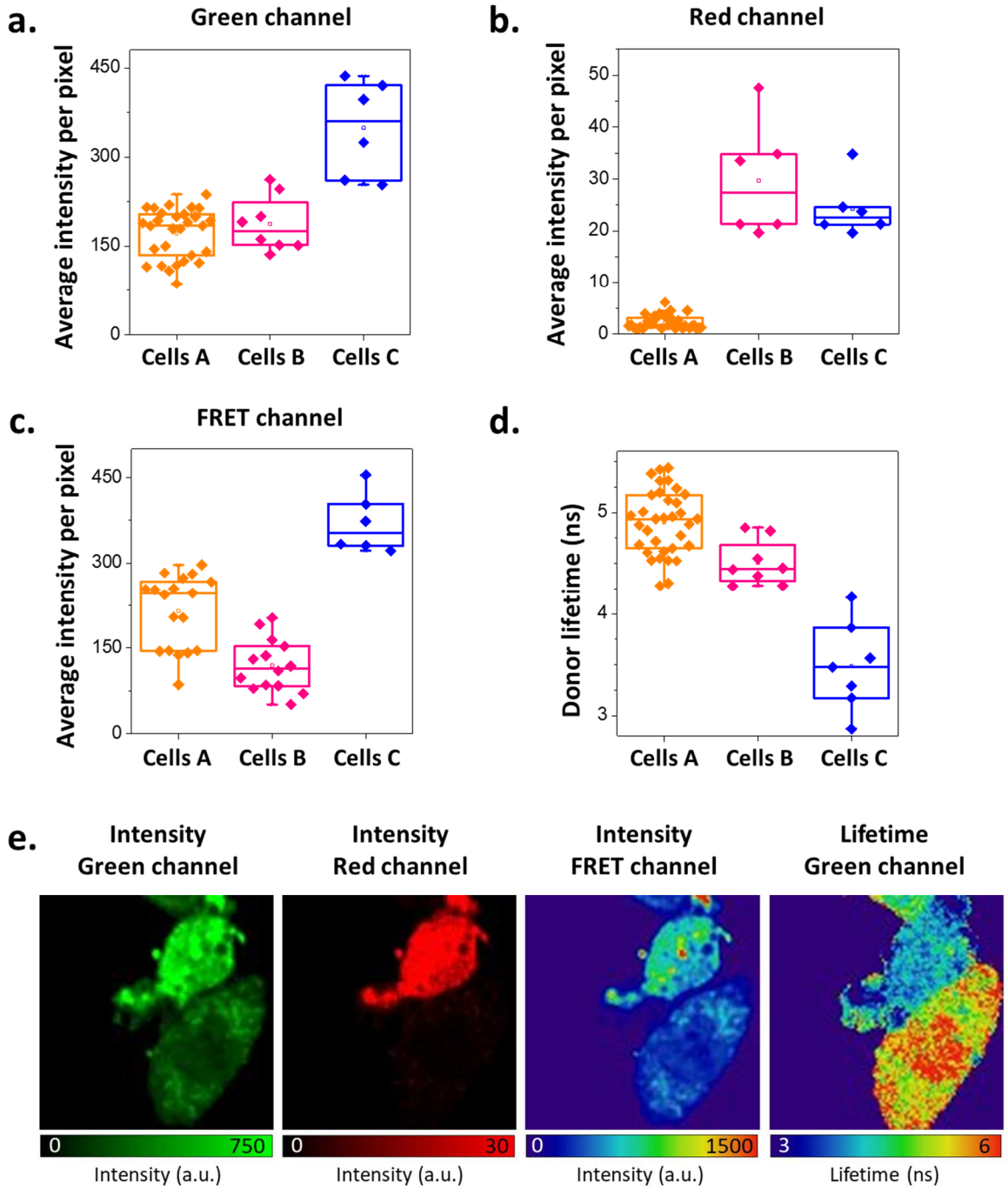

Figure 7. Intracellular FRET-based biosensor measurements and images. Box and whisker plots representing the average fluorescence intensity (**a**) in the green channel, (**b**) in the red channel, (**c**) in the FRET channel and (**d**) the fluorescence lifetime of the donor dye **5** in pixels from FLIM images containing Pep1-K5-**5**-labelled peptide in N2a cells. Boxes represent the 25 and 75%, with a horizontal bar showing the average value. Whiskers correspond to the minimum and maximum values. (**e**) Representative dual-color FLIM images containing two different types of cells, cell C (top) and cell A (below), according to p25 expression levels. The three images on the left represent the fluorescence intensities from the green, red and FRET channels. The right image represents the fluorescence lifetime of Pep1-K5-**5**.

As shown in Figure 7a, compared to cells expressing physiological levels of p25 (cells A and B), the binding of Pep1-K5-**5** to cells overexpressing p25 (cells C) resulted in a >2.5-fold increase in the emission intensity of the peptide biosensor in the green channel. This increase was associated with the higher concentration of p25 in cells overexpressing this protein, which upon interaction with Pep1-K5-**5** promoted an increase in the hydrophobicity of the local environment of the fluorescent probe and, therefore, increases its fluorescence emission. Importantly, this fluorescence increase successfully allowed us to distinguish between cells with different intracellular concentrations of p25. Furthermore, as expected, when the red channel fluorescence was studied (Figure 7b), low fluorescence levels were detected in non-transfected N2a cells (cells A), while similar levels of NIR fluorescence were detected on the cells transfected either with the pmiRFP670-N1 (cells B) or pmiRFP670-N-P25 plasmids (cells C). As a consequence of the energy transfer from the 9-amino-quinolimide labelled peptide Pep1-K5-**5** to p25-miRFP670, the intensity in the FRET channel, using compound **5** excitation wavelength but selecting the far-red emission channel (Figure 7c), was higher in the population of "C" cells than in the population of "A" cells, where FRET was not possible due to the absence of the FRET acceptor p25-miRFP670. Furthermore, when FRET was analyzed in the pmiRFP670-N1 transfected cells ("B" cells), the signal was absent since there was no miRFP670 protein fused to the p25 moiety available for energy transfer from the 9-amino-quinolimide labelled peptide Pep1-K5-**5** onto miRFP670.

The interaction of Pep1-K5-**5** with the p25-miRFP670 protein not only produced an increase in FRET fluorescence intensity, but more significantly produced a decrease on the fluorescence lifetime of Pep1-K5-**5**, which is an unequivocal feature of actual FRET, and is evidenced by FLIM microscopy. Figure 7d shows the fluorescence lifetime obtained from the green channel for cell populations A, B and C. The fluorescence lifetime of the donor quinolimide in the Pep1-K5-**5** biosensor approximately decreased from 4.9 or 4.5 in cells expressing physiological levels of p25, cells A and B respectively, to 3.7 ns in cells C, which represents an average FRET efficiency of 0.24 (estimated with respect to the lifetime of Pep1-K5-**5** in cells A). These results confirmed the presence of FRET between Pep1-K5-**5** and p25-miRFP670 in cells overexpressing p25, and, therefore,

demonstrated the intracellular binding between the CDK5-based peptide Pep1-K5-**5** and its regulatory partner p25. The significant decrease in the fluorescence lifetime of the peptide biosensor confirms the utility of our FRET based system to probe the CDK5/p25 interaction and to detect ectopic overexpression of p25. As expected, in the population of "B" cells, where only miRFP670 was expressed, no lifetime changes in the donor due to FRET were observed. Figure 7e shows a representative example of a dual color FLIM experiment in which two different types of cells were detected. In this example a cell is characterized by a high intensity in the red and the FRET channels and a low donor lifetime (cell C), whereas the other cell shows negligible intensity in the red and the FRET channel and a high donor lifetime (cell A). This indicates different p25 levels in these two cell populations.

To demonstrate the usefulness of the measurement system based on the interaction of Pep1-K5-**5** with the p25-miRFP670 in physio-pathological conditions, N2a cells transfected with the pmiRFP670-N-P25 plasmid (cells C) were either differentiated to neurites or treated with rosiglitazone, and then the donor lifetime of the sensor was compared to that found in the N2a untransfected cells (cells A) (Figure 8). The differentiation of N2a cells to neurites involves an increase in the endogenous levels of p25 that translated into an enhanced CDK5 activity [36]. Therefore, an increase in the lifetime could be expected due to competition between the increased levels in p25 in the differentiated neurites and the p25-miRFP670 protein for binding to the Pep1-K5-**5** probe. On the contrary, it has been described that in neuroblastoma cells, incubation with thiazolidinediones such as rosiglitazone [37] increases the degradation rate of p25 decreasing its intracellular levels. Following the same rationale, this should translate in a decrease in the fluorescence lifetime of C cells treated with rosiglitazone. Our results confirmed that the sensor can be used to follow expression levels of p25 in physiological conditions (differentiation to neurites) or after pharmacological treatment (incubation with rosiglitazone), validating our measurement system in cells cultures in response to intracellular changes of p25.

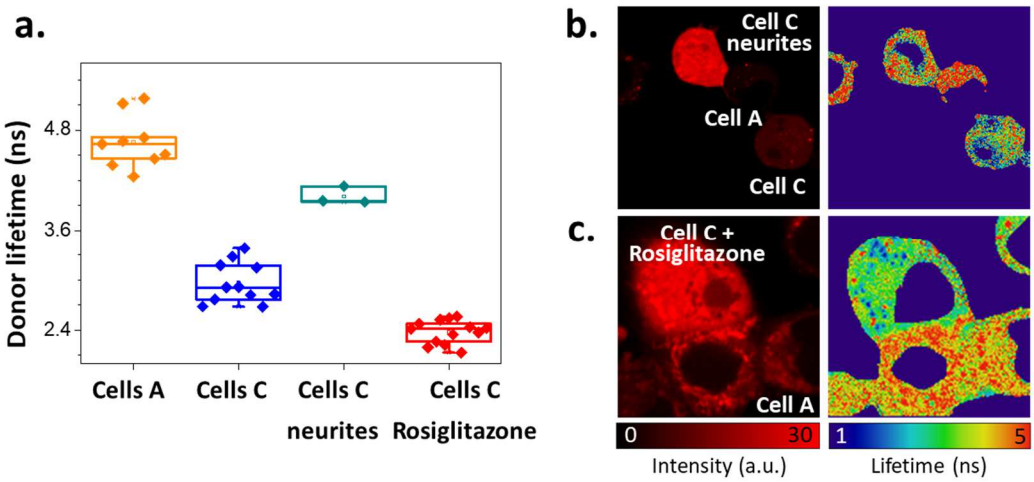

Figure 8. Intracellular FRET-based biosensor measurements in physio-pathological conditions. (**a**) Box and whisker plots representing the fluorescence lifetime of the donor dye **5** in pixels from FLIM images containing Pep1-K5-**5**-labelled peptide in N2a cells. Boxes represent the 25 and 75%, with a horizontal bar showing the average value. Whiskers correspond to the minimum and maximum values. N2a cells were transfected with the pmiRFP670-N-P25 plasmid (cells C) and were either differentiated to neurites (Cells C neurites) or treated with rosiglitazone (Cells C rosiglitazone). Cells A were untransfected N2a cells. (**b** and **c**) Representative dual-color FLIM images (left column: fluorescence intensity from the red channel; right column: fluorescence lifetime of Pep1-K5-**5**) containing (**b**) three different types of cells, cell C differentiated to neurites (top), cell A (middle) and cell C undifferentiated (below), or (**c**) two different types of cells, cell C treated with rosiglitazone (top) and cell A (below), according to p25 expression levels.

4. Conclusions

The results herein described illustrate the remarkable potential of highly solvatochromic and fluorogenic 9-(substituted amino)-quinolimide-based fluorophores, and particularly 9-azetidinyl-quinolimides, as tools for fluorescence peptide labelling, and to obtain biosensors of cell cycle regulators. Specifically we describe the design and synthesis of CDK5-based peptide biosensors labelled with 9-methylamino- or 9-azetidinyl-quinolimides, which showed *in vitro* µM affinity for p25, the regulatory partner of CDK5. We have further shown that the 9-azetidinyl-quinolimide labelled biosensor (Pep1-K5-**5**) colocalized with p25 in U87 glioblastoma cells. Finally we have developed a FRET strategy combining our peptide biosensor and ectopic expression of the NIR fluorescent miRFP670-p25 fusion protein, which has enabled to formally demonstrate the interaction between the Pep1-K5-**5** biosensor and ectopically expressed miRFP670-p25 in neuroblastoma N2a

cells. Our studies have shown that the FRET response is correlated with p25 levels. Moreover, the implementation of this system opens the door to its use for the *in cellulo* screening of libraries of compounds for identification of CDK5/p25 modulators of therapeutic interest.

Conflict of interest

The authors have no conflicts of interest to declare.

Acknowledgements

This work was supported by the Ministerio de Ciencia e Innovación/Agencia Estatal de Investigación grants FU2015-67284-R and PID2019-104366RB-C22, the Ministerio de Ciencia e Innovación/Agencia Estatal de Investigación/European Regional Development Fund grant CTQ2017-85658-R, and the CSIC grant 201580E073, and the CNRS (Centre National de la Recherche Scientifique). We acknowledge the MRI imaging facility (Montpellier, France), a member of the national infrastructure France-BioImaging.

Supplementary Material

Supplementary material to this article can be found online at

References

[1] L.-H. Tsai, I. Delalle, V.S. Caviness, Jr., T. Chae, E. Harlow, P35 is a neural-specific regulatory subunit of cyclin-dependent kinase 5, Nature, 371(1994) 419-23.

[2] R. Roufayel, N. Murshid, CDK5: Key Regulator of Apoptosis and Cell Survival, Biomedicines, 7(2019).

[3] M. Peyressatre, C. Prevel, M. Pellerano, M.C. Morris, Targeting cyclin-dependent kinases in human cancers: from small molecules to Peptide inhibitors, Cancers, 7(2015) 179-237.
[4] R. Dhavan, L.H. Tsai, A decade of CDK5, Nature reviews Molecular cell biology, 2(2001) 749-59.
[5] G. Kusakawa, T. Saito, R. Onuki, K. Ishiguro, T. Kishimoto, S. Hisanaga, Calpain-dependent proteolytic cleavage of the p35 cyclin-dependent kinase 5 activator to p25, J Biol Chem, 275(2000) 17166-72.
[6] M.-s. Lee, Y.T. Kwon, M. Li, J. Peng, R.M. Friedlander, L.-H. Tsai, Neurotoxicity induces cleavage of p35 to p25 by calpain, Nature 405(2000) 360-4.
[7] S.B. Shelton, G.V.W. Johnson, Cyclin-dependent kinase-5 in neurodegeneration, J Neurochem, 88(2004) 1313-26.
[8] A. Camins, E. Verdaguer, J. Folch, A.M. Canudas, M. Pallas, The role of CDK5/P25 formation/inhibition in neurodegeneration, Drug News Perspect, 19(2006) 453-60.
[9] Z.H. Cheung, N.Y. Ip, Cdk5: a multifaceted kinase in neurodegenerative diseases, Trends Cell Biol, 22(2012) 169-75.
[10] L.-F. Lau, M.K. Ahlijanian, Role of cdk5 in the pathogenesis of Alzheimer's disease, Neurosignals, 12(2003) 209-14.
[11] J. Kanungo, Special Issue on "Cdk5 and Brain Disorders": Prologue, Brain Disord Ther, Suppl 1(2012) 1-5.
[12] J.P. Brion, A.M. Couck, Cortical and brainstem-type Lewy bodies are immunoreactive for the cyclin-dependent kinase 5, Am J Pathol, 147(1995) 1465-76.
[13] E. Rubio de la Torre, B. Luzon-Toro, I. Forte-Lago, A. Minguez-Castellanos, I. Ferrer, S. Hilfiker, Combined kinase inhibition modulates parkin inactivation, Hum Mol Genet, 18(2009) 809-23.
[14] M.D. Nguyen, J.-P. Julien, Cyclin-Dependent Kinase 5 in amyotrophic lateral sclerosis, Neurosignals, 12(2003) 215-20.
[15] D.A. Meyer, M.I. Torres-Altoro, Z. Tan, A. Tozzi, M. Di Filippo, V. DiNapoli, et al., Ischemic stroke injury is mediated by aberrant Cdk5, J Neurosci, 34(2014) 8259-67.
[16] K. Pozo, J.A. Bibb, The Emerging Role of Cdk5 in Cancer, Trends Cancer, 2(2016) 606-18.
[17] A. Shupp, M.C. Casimiro, R.G. Pestell, Biological functions of CDK5 and potential CDK5 targeted clinical treatments, Oncotarget, 8(2017) 17373-82.
[18] A. Catania, S. Urban, E. Yan, C. Hao, G. Barron, J. Allalunis-Turner, Expression and localization of cyclin-dependent kinase 5 in apoptotic human glioma cells, Neuro-oncology, 3(2001) 89-98.
[19] R. Liu, B. Tian, M. Gearing, S. Hunter, K. Ye, Z. Mao, Cdk5-mediated regulation o the PIKE-A-Akt pathway and glioblastoma cell invasion, Proc Natl Acad Sci U S A, 105(2008) 7570-5.
[20] R. Yushan, G. Roodrajeetsing, C. Wenjie, D. Yiwu, Z. Tengfei, W.M. Madushi, et al., Insights into the clinical value of cyclin-dependent kinase 5 in glioma: a retrospective study, World J Surg Oncol, 13(2015) 223.
[21] G.S. Loving, M. Sainlos, B. Imperiali, Monitoring protein interactions and dynamics with solvatochromic fluorophores, Trends Biotechnol, 28(2010) 73-83.
[22] A.S. Klymchenko, Solvatochromic and Fluorogenic Dyes as Environment-Sensitive Probes: Design and Biological Applications, Accounts of chemical research, 50(2017) 366-75.
[23] J.A. González-Vera, F. Fueyo-González, I. Alkorta, M. Peyressatre, M.C. Morris, R. Herranz, Highly solvatochromic and tunable fluorophores based on a 4,5-quinolimide scaffold: novel CDK5 probes, Chem Commun 52(2016) 9652-5.
[24] F. Fueyo-González, J.A. González-Vera, I. Alkorta, L. Infantes, M.L. Jimeno, P. Aranda, et al., Environment-Sensitive Probes for Illuminating Amyloid Aggregation In Vitro and in Zebrafish, ACS Sens, 5(2020) 2792-9.
[25] N.D. Amin, W. Albers, H.C. Pant, Cyclin-dependent kinase 5 (cdk5) activation requires interaction with three domains of p35, Journal of neuroscience research, 67(2002) 354-62.

[26] D.M. Shcherbakova, M. Baloban, A.V. Emelyanov, M. Brenowitz, P. Guo, V.V. Verkhusha, Bright monomeric near-infrared fluorescent proteins as tags and biosensors for multiscale imaging, Nature communications, 7(2016) 12405.
[27] J. Schindelin, I. Arganda-Carreras, E. Frise, V. Kaynig, M. Longair, T. Pietzsch, et al., Fiji: an open-source platform for biological-image analysis, Nature methods, 9(2012) 676-82.
[28] B. Štefane, F. Požgan, I. Sosič, S. Gobec, A microwave-assisted nucleophilic substitution reaction on a quinoline system: the synthesis of amino analogues of nitroxoline, Tet Lett, 53(2012) 1964-7.
[29] C. Tarricone, R. Dhavan, J. Peng, L.B. Areces, L.-H. Tsai, A. Musacchio, Structure and regulation of the CDK5-p25nck5a complex, Mol Cell, 8(2001) 657-69.
[30] M. Mapelli, L. Massimiliano, C. Crovace, M.A. Seeliger, L.H. Tsai, L. Meijer, et al., Mechanism of CDK5/p25 binding by CDK inhibitors, Journal of medicinal chemistry, 48(2005) 671-9.
[31] L. Kurzawa, M. Pellerano, J.B. Coppolani, M.C. Morris, Fluorescent peptide biosensor for probing the relative abundance of cyclin-dependent kinases in living cells, PloS one, 6(2011) e26555.
[32] M.C. Morris, J. Depollier, J. Mery, F. Heitz, G. Divita, A peptide carrier for the delivery of biologically active proteins into mammalian cells, Nat Biotech, 19(2001) 1173-6.
[33] L. Kurzawa, M. Pellerano, M.C. Morris, PEP and CADY-mediated delivery of fluorescent peptides and proteins into living cells, Biochim Biophys Acta, 1798(2010) 2274-85.
[34] D.M. Shcherbakova, V.V. Verkhusha, Near-infrared fluorescent proteins for multicolor in vivo imaging, Nature methods, 10(2013) 751-4.
[35] J. Zhang, H. Li, T. Zhou, J. Zhou, K. Herrup, Cdk5 levels oscillate during the neuronal cell cycle: Cdh1 ubiquitination triggers proteosome-dependent degradation during S-phase, J Biol Chem, 287(2012) 25985-94.
[36] T. Kawauchi, Cdk5 regulates multiple cellular events in neural development, function and disease, Development, growth & differentiation, 56(2014) 335-48.
[37] D.H. Cho, E.J. Lee, K.J. Kwon, C.Y. Shin, K.H. Song, J.H. Park, et al., Troglitazone, a thiazolidinedione, decreases tau phosphorylation through the inhibition of cyclin-dependent kinase 5 activity in SH-SY5Y neuroblastoma cells and primary neurons, Journal of neurochemistry, 126(2013) 685-95.

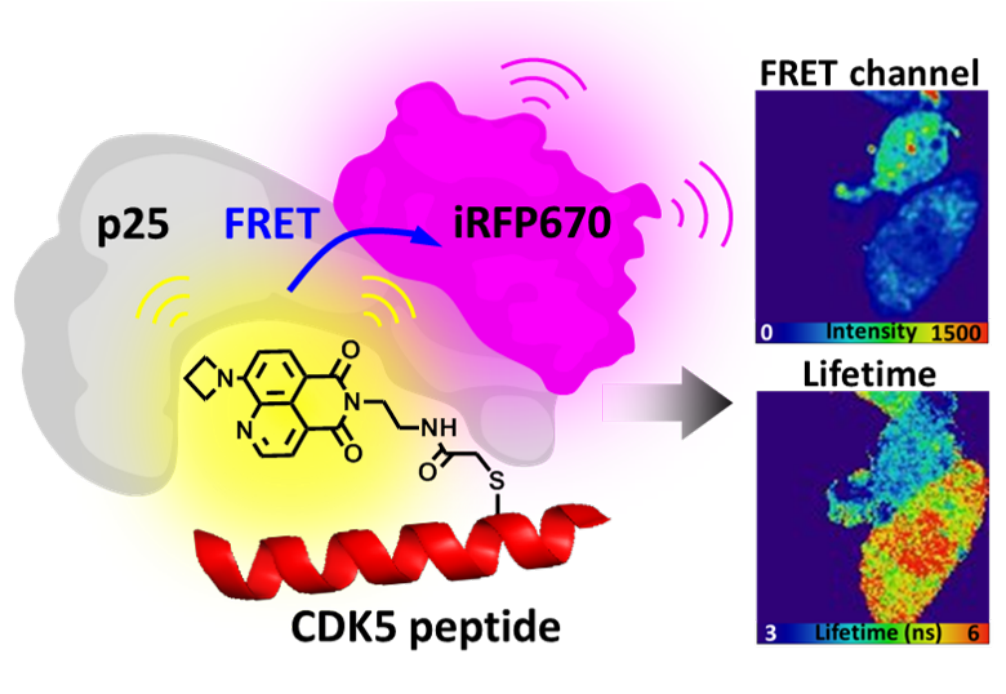
p25
FRET
iRFP670
CDK5 peptide
FRET channel
0
Intensity
1500
Lifetime
3
Lifetime (ns)
6